PROCEEDINGS, 42nd Workshop on Geothermal Reservoir Engineering
Stanford University, Stanford, California, February 13-15, 2017
SGP-TR-209

Monitoring Geothermal Reservoir Depletion Using Time-Dependent Tomography

Najwa Mhana[1], Bruce R. Julian[1], Gillian R. Foulger[1], and Andrew E. Sabin[2]

[1]Dept. of Earth Sciences, Durham University, Durham DH1 3LE, United Kingdom

[2]U. S. Navy Geothermal Program Office, China Lake, CA 93555

najwa.mhana@durham.ac.uk; b.r.julian@durham.ac.uk; g.r.foulger@durham.ac.uk; andrew.sabin@navy.mil

Keywords: Seismic tomography; temporal change; Coso;

ABSTRACT

Temporal changes in seismic wave speeds in geothermal areas have been detected using time-dependent seismic tomography. However, despite the potential value of such measurements for monitoring exploited geothermal reservoirs, most reports of changes in wave speeds are of questionable reliability. This is because changes in *calculated* structure are expected, even if the *real* structure did not change, as a result of different experimental conditions and observational errors from epoch to epoch.

The difficulties in detecting true changes in seismic wave speeds can be greatly reduced by inverting data from different epochs simultaneously, imposing "regularization" constraints to minimize the differences between derived models. This method suppresses spurious changes that are not required by the data.

We report on the application of this method using the program *tomo4d* to data from the exploited Coso geothermal area in southeastern California. The Coso geothermal area is the seventh largest exploited geothermal area in the world. It is 28 km^2 in area, and has a water-dominated reservoir with temperatures up to ~ 345ºC. It has been under production for two decades, and now has ~ 180 boreholes up to 4 km deep and produces 300 Mw of electricity, sufficient for the needs of ~1 million people. We performed tomographic inversions for the years 1996, 2006, 2007, 2008, 2010, and 2012, and studied the epochs 1996-2006 and 2007-2012 in detail. The wave speeds Vp and Vs, and the ratio Vp/Vs, mostly increased during the first epoch in the geothermal field but were more varied during the second epoch. We conclude that different parts of the field have different reservoir characteristics, and that operational activities changed with time. These may have involved increasing water saturation in some areas as a result of increased water injection in recent years.

1. INTRODUCTION

The mechanical properties of porous rocks depend, among other things, upon the properties of the pore fluids, and thus should change in response to geothermal exploitation and to natural processes. Indeed, strong and easily detectable changes in the seismic wave speeds reportedly occur at some heavily exploited geothermal fields, such as The Geysers in northern California (Gunasekera *et al.,* 2003). The Geysers is exceptional, however, and at most fields temporal changes are likely to be weak and challenging to identify with certainty.

Temporal changes in the structure of geothermal areas have until now been investigated by applying conventional tomographic techniques to invert seismic wave arrival-time data for different epochs independently, and assuming that differences in the resulting models reflect real temporal structural changes. Unfortunately, changes between derived models are expected even if the structure did not actually change, due to differences in seismic ray distributions and to inevitable observational errors. Thus, it remains open to question whether the weak changes in structure sometimes reported at geothermal areas are real.

It is possible to overcome these difficulties by inverting data sets from different epochs simultaneously, imposing "regularization" constraints to minimize the differences between derived models for different epochs. This approach requires solving systems of linear equations whose order is twice that required for independent inversion. However, sparseness of the matrices involved makes possible optimizations that largely compensate for this disadvantage. In this paper, we use this approach, as implemented in the local-earthquake tomography program *tomo4d* (Julian and Foulger, 2010). We apply it to assess possible temporal changes at the exploited Coso geothermal area, eastern California.

tomo4d takes advantage of the sparse structure of the relevant matrices to achieve significant computational efficiencies. It also incorporates significant improvements over previous local-earthquake tomography programs. For example, it performs true ray tracing through 3D structures (Julian and Gubbins, 1977). Tests using synthetic data verify that *tomo4d* suppresses artificial temporal variations in seismic-wave speed (Julian and Foulger, 2010).

The difficulties in measuring temporal changes are consequences of the small amount of information contained in any real seismic data set compared with the information required to specify fully a detailed three-dimensional model of Earth structure. There will always be an infinite number of significantly different 3D models that fit observations within their uncertainties, and examining particular tomographic models often sheds little light on the true structure and processes within the Earth. Our

approach, of finding the smallest temporal changes consistent with observation, attempts to test hypotheses by falsifying possible models, as advocated by Tarantola (2006).

The commercially exploited Coso geothermal area (Figure 1), located near the southwestern corner of the Basin and Range Province in southeastern California, is an area of high microearthquake activity, both natural and induced. The geothermal field lies on the U.S. Naval Air Weapons Test Site at China Lake, and the seismometer network operated by the Geothermal Program Office of the US Navy. It records thousands of small, local earthquakes each year.

Foulger (2007) performed independent local-earthquake tomography inversions of high-quality subsets of data from each of the nine years 1996-2004, and found evidence of an irregular reduction of the wave-speed ratio V_P/V_S in the upper ~2 km of the geothermal field. It was irregularities in the apparent temporal changes in V_P/V_S found in this study that motivated developing *tomo4d*. In the present study we processed data for the years 1996, 2006, 2007, 2008, 2010 and 2012.

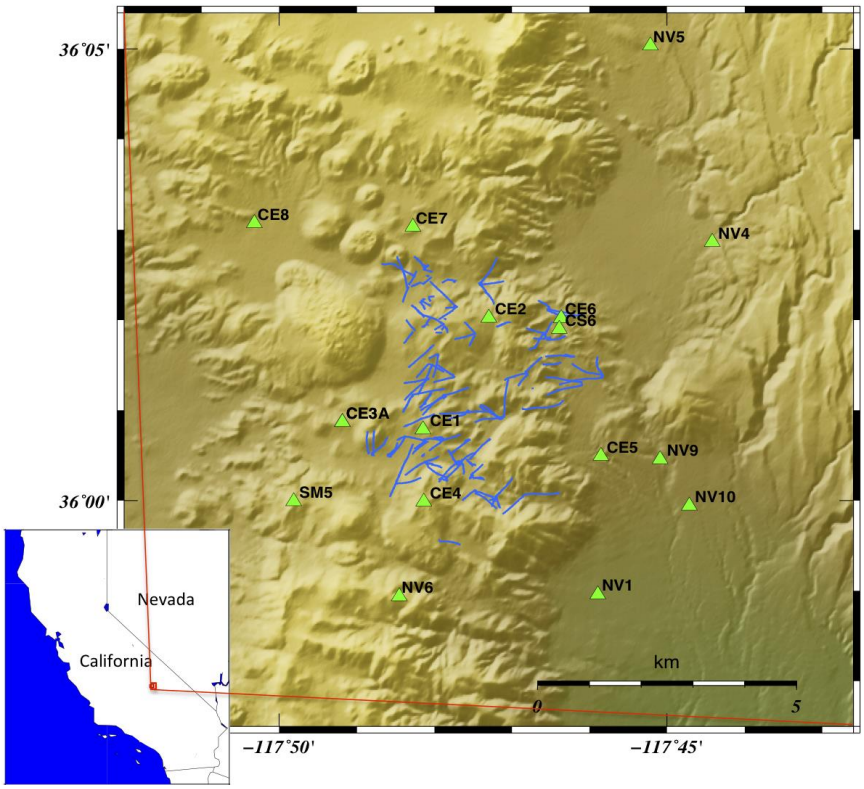

Figure 1: Map of the Coso geothermal area showing shaded topographic relief. Green triangles: seismometer stations; blue lines: surface projections of geothermal wells. These indicate the location of the geothermal field. The inset map shows the location of the main map in California.

2. DATA ANALYSIS

2.1 Selecting Data and Damping Parameters

The datasets selected for inversion include a few hundred of the best-recorded earthquakes for each year, well distributed throughout the study volume. To choose these, we subdivided the study volume into 200 cubes (Figure 2), and selected the 10 events of highest quality in each cube, ranking events by the number of arrival-time measurements, smallness of the root-mean-square arrival-time residuals, smallness of the azimuthal gap between seismometers, and event magnitude. The final datasets contained 680, 570, 512, and 504 earthquakes for 2007, 2008, 2010, and 2012 respectively. In order to investigate longer-period variations, sets of data from the years 1996 and 2006 were used.

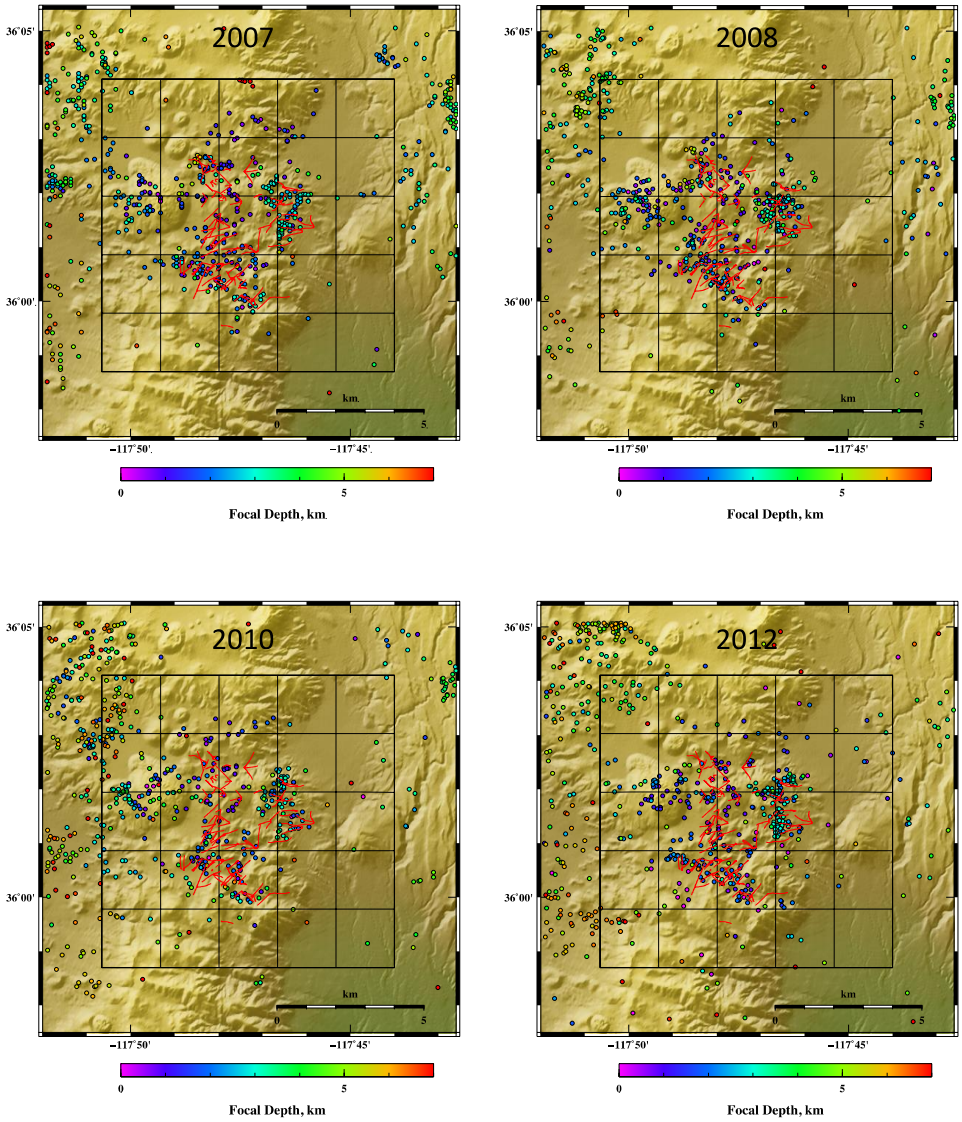

Figure 2: Shaded-relief maps of the Coso geothermal area, showing earthquakes analyzed for the years 2007, 2008, 2010 and 2012, color-coded by focal depth, and the 10 x 10 x 8 km grid on which the tomographic models are defined. Borehole paths are in red.

The Geothermal Program Office of the US Navy measured the *P*- and *S*-phase arrival times automatically for the events from 1996, 2006 and 2007. For the years 2008, 2010, and 2012, we measured arrival times manually, using the interactive program *epick*. The accuracy with which arrival times could be measured is ~0.01 s for *P* phases and ~0.3 s for *S* phases.

tomo4d uses a multi-component objective function to control the magnitudes of perturbations made to event origins, seismic wave speeds and inter-epoch wave-speed differences. To choose values for the parameters ε_{Origin}, $\varepsilon_{Velocity}$, and ε_{Epoch}that control this "damping" process, we performed single-iteration inversions using a variety of values and the resulting changes in goodness of fit and origin- and model perturbations were examined. Figure 3 shows the results of the tests, conducted using data for 1996 and 2006. The chosen damping values were then tested for five iterations to ensure the optimal values had been selected.

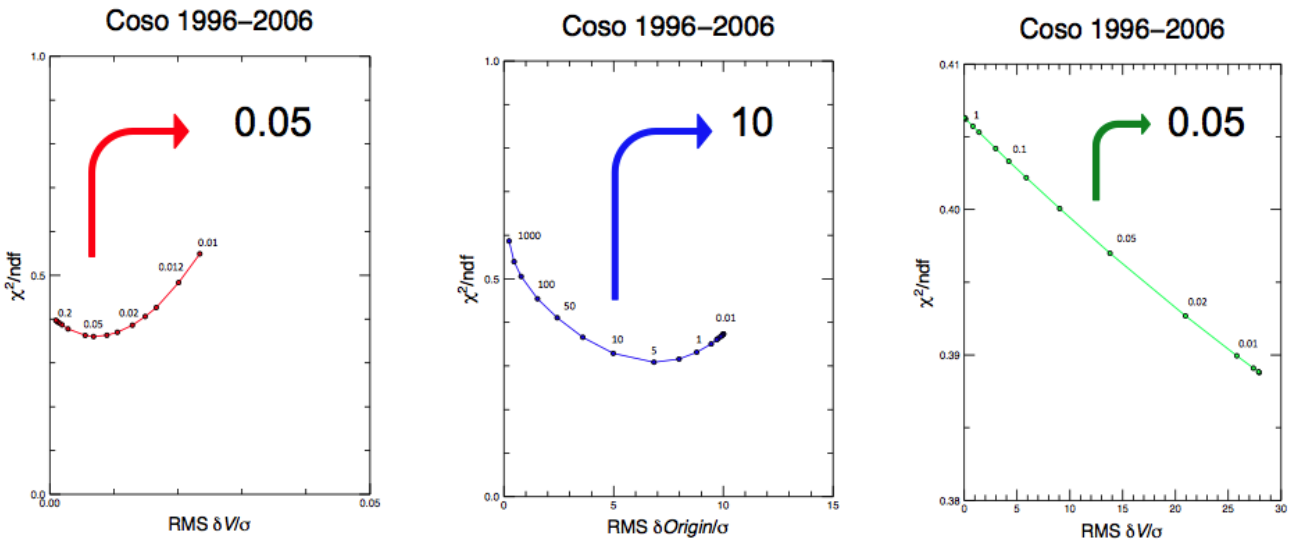

Figure 3: The trade-off damping curves for wave-speed damping $\varepsilon_{Velocity}$ (left), event origin ε_{Origin} (middle), and inter-epoch ε_{Epoch} (right) for models of the Coso geothermal area derived from data for 1996 and 2006. The highlighted values are the chosen optimal damping values.

2.2 Hit Counts and Quality of the Results

The numbers of ray paths passing near each node of the model grid were plotted as ray-density maps (Figure 4) in order to illustrate the quality of the sampling. The best-sampled area for the years 2007 and 2012 is the main geothermal field down to 1 km b.s.l., because of the high level of induced seismicity within the geothermal area around the production wells. At 2 km b.s.l. sampling is poorer because seismicity decreases with depth. Ray-path density for V_s is almost as good as for V_p, because of the large number of *S* measurements. We interpret the results for the best-sampled area.

The reduction in data residuals for the inversions of 2007 and 2012 are given as histograms in Figure 5. The final RMS travel-time residual for the 2007 data was ~0.04 s for *P*-phases and ~0.07 s for *S*. For the 2012 data the corresponding values were ~0.03 s and ~0.04 s. The higher final RMS for *S* residuals shows that the V_p/V_s model is not resolved as well as the V_p model.

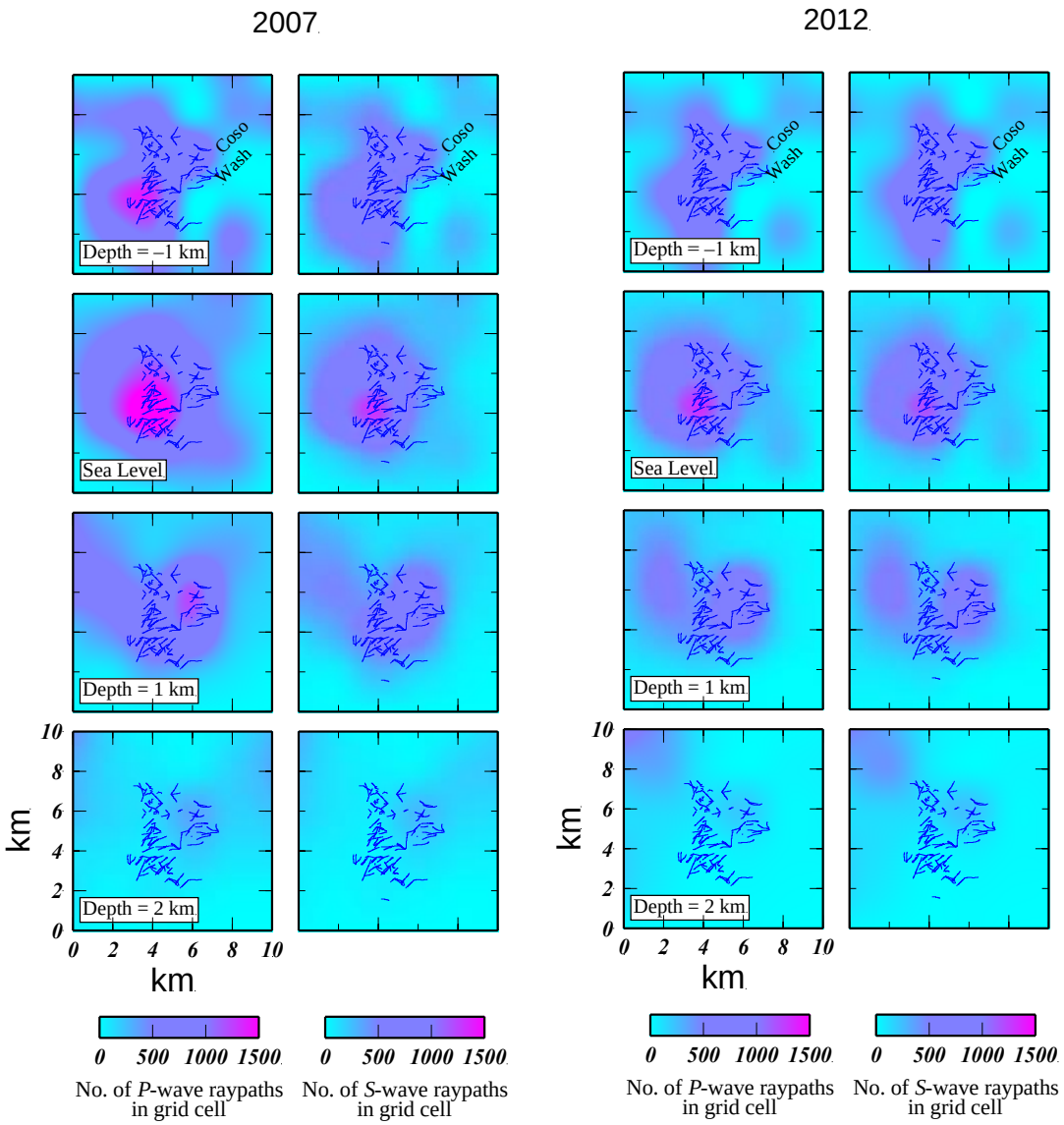

Figure 4: Hit-count maps showing the best-sampled areas in the study volume at different depths for 2007 (left pair of columns, left *P*, right *S*) and for 2012 (right).

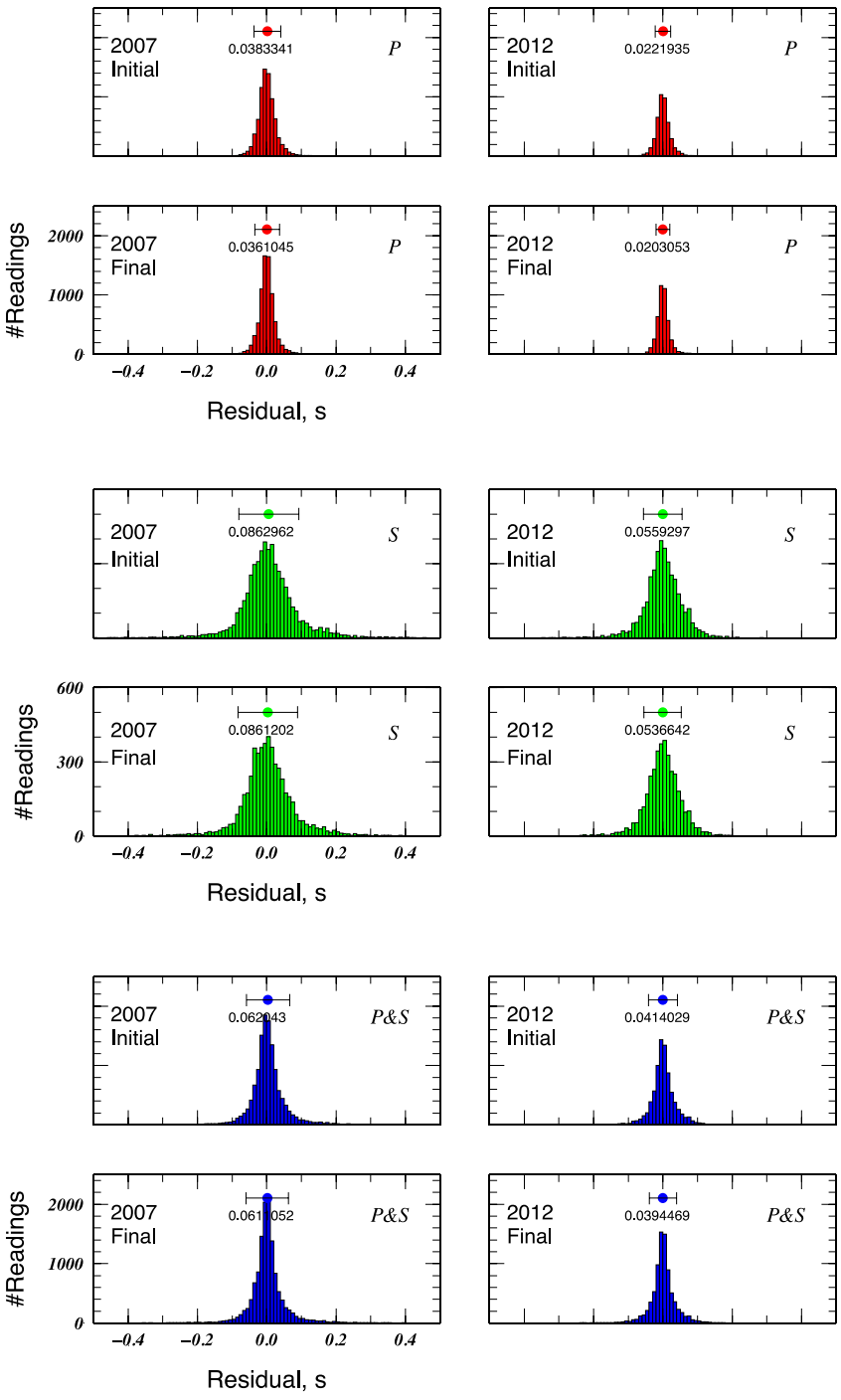

Figure 5: Histograms of the initial and final arrival-time residuals (red) for *P*-phases, (green) for *S*-phases and (blue) for both *P* and *S*, for the inversions of 2007 and 2012 data using program *simul2000A*. The coloured circle at the top of each histogram indicates the mean residual and the error bar shows the spread around the mean value. The number below the circle gives the RMS residual.

3. RESULTS

3.1 Structural Changes Between 1996-2006

Between 1996 and 2006, changes in V_p and V_s comprise mainly an increase of ~2% in the upper two kilometres within the geothermal field (Figure 6). The anomaly changes sign and becomes weaker below sea level, with a decrease of ~1% within the geothermal field except for an increase in V_p in the eastern part at a depth of 1 km b.s.l. Changes in V_p/V_s between 1996 and 2006 are a ~2% increase within the geothermal field as the result of an increase in V_s and a stronger increase in V_p near sea level and 1 km a.s.l. (Figure 6, red circles).

Possible factors that could cause increases in V_p and V_s are: a) increase in water saturation, b) decrease in pore pressure, c) drying of minerals, and d) temperature decrease. It is known that the top 1-2 km of the Coso geothermal field is heavily depleted in water. Thus a) can be ruled out. On the other hand, the Coso geothermal reservoir is known to be depleting and thus b) - d) are expected. In all cases b) - d), a larger increase in V_s than V_p is expected, and thus a decrease in V_p/V_s. This is not observed and instead a large increase in V_p is seen along with an increase in V_p/V_s. The explanation for this unexpected observation must lie in different relative effects on V_p and V_s than expected. More detailed study of this in future is warranted.

Two volumes where V_p/V_s decreased are as follows. At 1 km a.s.l. in the northeastern part of the geothermal field (Figure 6, green circles) there is a small increase in V_p and a stronger increase in V_s. This could be caused by pore pressure decrease and drying of minerals (Table 1, green circles). A second decrease in V_p/V_s occurs in the southwestern part of the geothermal field at 1 km b.s.l. (Figure 6, blue circles). This results from decrease in both V_p and V_s with the decrease in V_p being stronger than in V_s. This is expected as a result of depletion in geothermal reservoirs and steam replacing water (Table 1, blue circles).

3.2 Structural Changes Between 2007-2012

The change detected between 2007 and 2012 is significantly different from the earlier epoch. Between 2007 and 2012, the changes in V_p and V_s are reversed and a general decrease of ~1% down to 1 km b.s.l. is detected. In some peripheral volumes, V_p increases (Figure 7, red circles). These are the northeastern part of the geothermal field at 1 km a.s.l., the east and southeastern part at sea level, and the southwestern part at 1 km b.s.l. These three anomalies correlate with an increase in V_p/V_s.

Increased water saturation, drying of minerals and pore pressure decrease can cause V_p to increase but only water saturation causes V_p/V_s to increase (Table 2). Increased water injection activity in recent years may explain the increased V_p/V_s in these areas. The reversal in sign of the main anomaly is surprising and it suggests a change in operational activity.

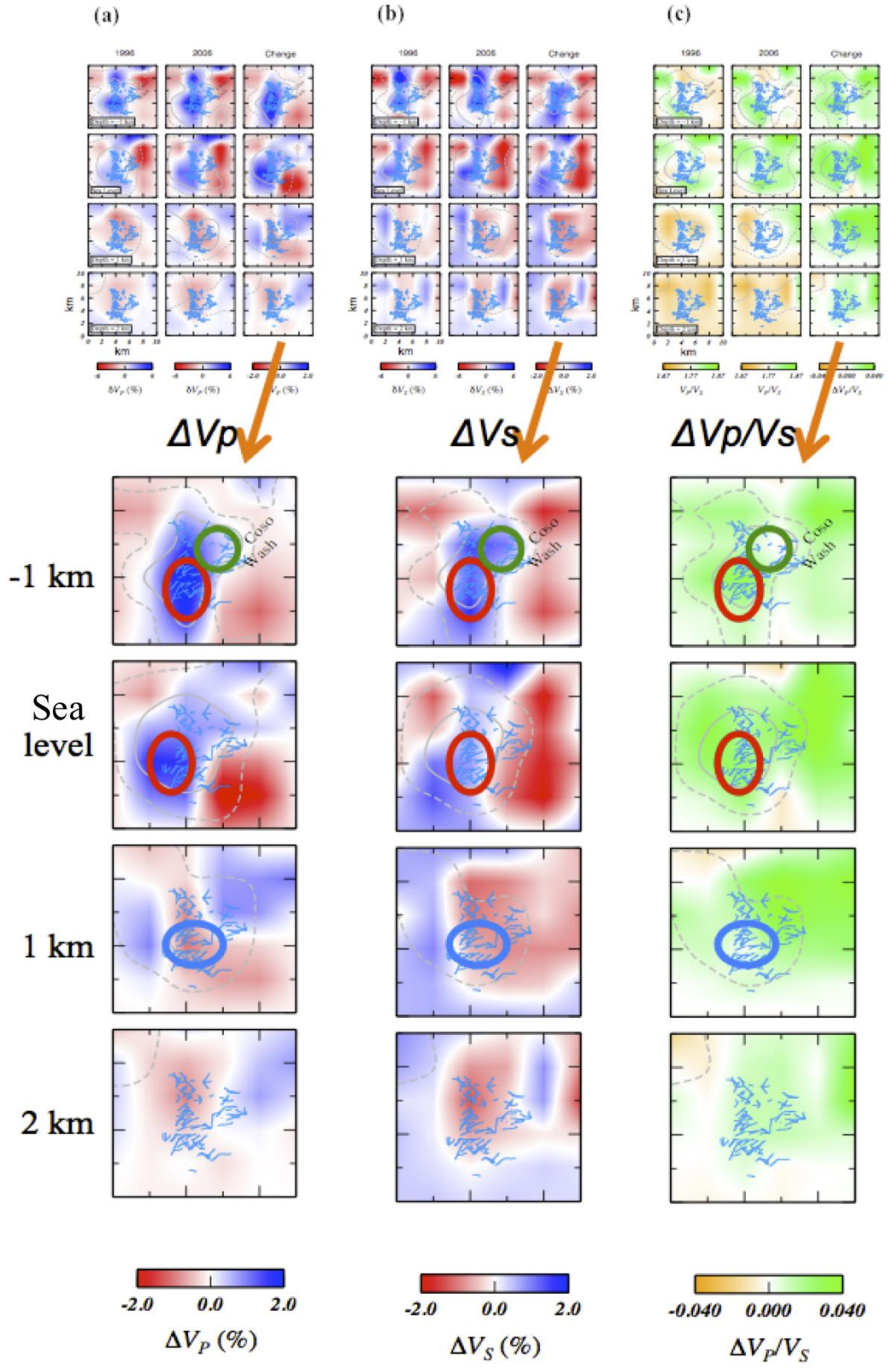

Figure 6. Top: (a) Structure for the Coso geothermal area obtained from inversions for 1996 (left panel) and 2006 (middle panel) along with the change between these two years (right panel) for V_p. (b) same as (a) for V_s and, (c) same as (a) for V_p/V_s. Solid and dashed grey lines are the 500- and 150-hit-count contours respectively. Bottom: enlargements of the change panels showing only the change in *Vp* (left), *Vs* (middle) and *Vp/Vs* (right) between 1996 and 2006. Green, red and blue circles indicate interpreted areas in the text.

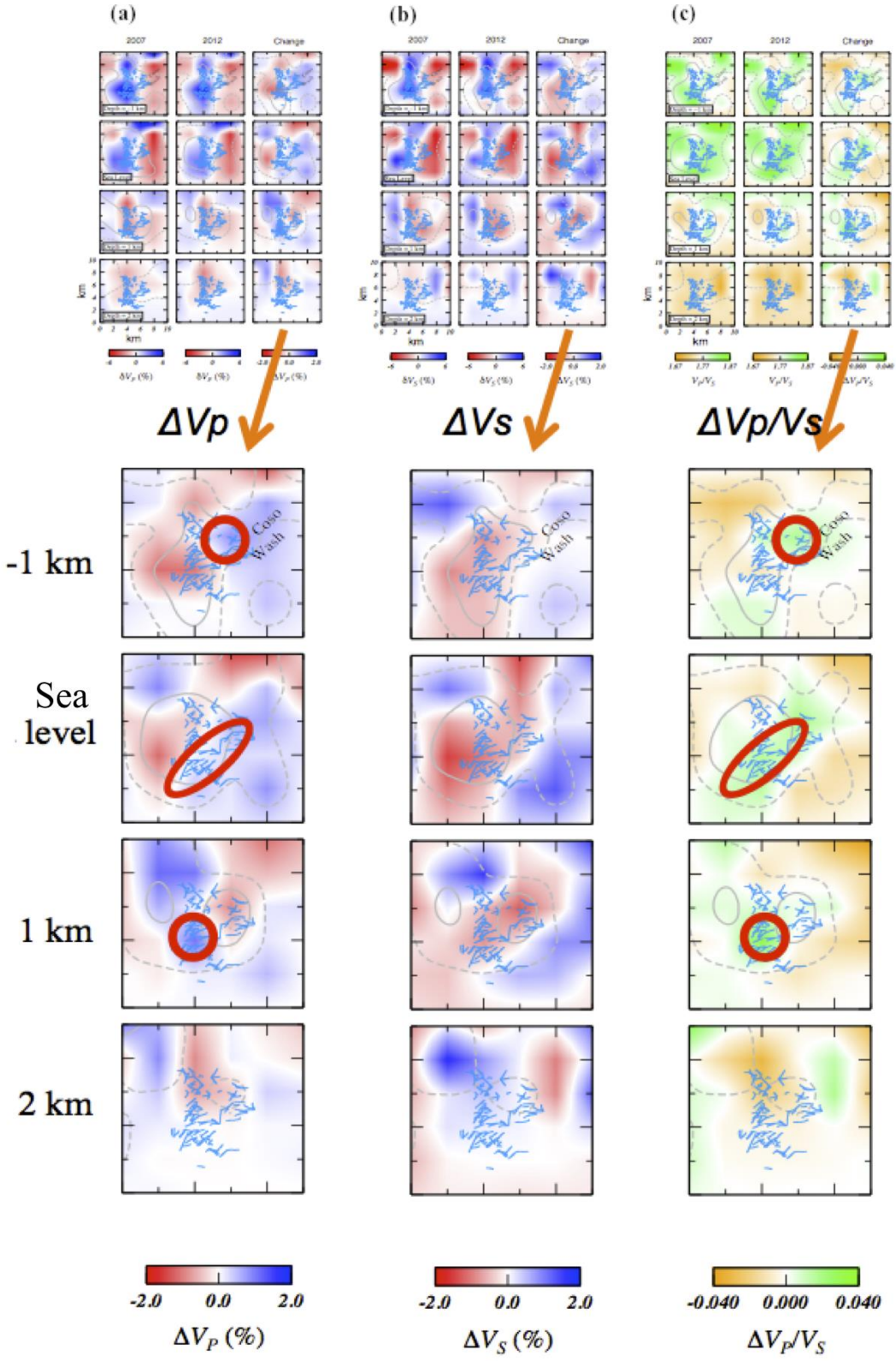

Figure 7. Same as Figure 6 for the years 2007-2012.

Table 1. The effects on V_p, V_s and V_p/V_s of processes that occur in geothermal areas. Large arrows indicate the dominant effects, and small arrows indicate weaker or negligible effects. Coloured circles indicate effects discussed in the text.

	V_p	V_s	V_p/V_s
Water saturation	↑	–	↑
Pressure increase and fracturing	↓	↓	↑
Pore pressure decrease	↑	↑	↓
Drying of minerals	↑	↑	↓
Temperature decrease	↑	↑	↓
Steam replacing water	↓	↓	↓

Table 2. Same as Table 2 with red circles indicating effects discussed in the text.

	V_p	V_s	V_p/V_s
Water saturation	↑	–	↑
Pressure increase and fracturing	↓	↓	↑
Pore pressure decrease	↑	↑	↓
Drying of minerals	↑	↑	↓
Temperature decrease	↑	↑	↓
Steam replacing water	↓	↓	↓

3. CONCLUSION

While the main structural change between 1996-2006 is consistent with water depletion and drying of minerals, after 2007 these trends appear to have reversed and changes detected are consistent with replenishment of the reservoir. Further work is needed to explore possible correlations between operations and the seismic results. Additional inversions for different epochs, selected on the basis of operational changes, may provide additional information.

REFERENCES

Evans, J. R., D. Eberhart-Phillips, and C. H. Thurber (1994), User's manual for SIMULPS12 for imaging V_P and V_P/V_S, a derivative of the Thurber tomographic inversion SIMUL3 for local earthquakes and explosions, Open-file *Report 94-431*, 142 pp., US Geological Survey.

Gunasekera, R. C., G. R. Foulger, and B. R. Julian (2003), Reservoir depletion at The Geysers geothermal area, California, shown by four-dimensional seismic tomography, J. Geophys. Res., **108**(B3), 2134,doi:2110.1029/2001JB000638.

Foulger, G. R., B. R. Julian, A. M. Pitt, D. P. Hill, P. E. Malin, and E. Shalev (2003), Three-dimensional crustal structure of Long Valley caldera, California, and evidence for the migration of CO_2 under Mammoth Mountain, *J. Geophys. Res.*, **108**(B3), 2147,doi:2110.1029/2000JB000041.

Foulger, G. R. (2007), Report to the U.S. Geological Survey on time-dependent seismic tomography of the Coso geothermal area, Inyo County, CA covering the years 1996-2006, Technical Rep., iv+119 pp, U.S. Geological Survey, Menlo Park, California.

Julian, B. R., and D. Gubbins (1977), Three-dimensional seismic ray tracing, *J. Geophys.*, **43**(1/2), 95-113.

Julian, B. R., G. R. Foulger, K. Richards-Dinger, and F. Monastero, Time-dependent seismic tomography of the Coso geothermal area, 1996-2004, *Proceedings*, 31st Workshop on Geothermal Reservoir Engineering, Stanford University, Stanford, CA (2006).

Julian, B. R., and G. R. Foulger (2010), Time-dependent seismic tomography, *Geophys. J. Int.*, **182**(3), 1327-1338.

Tarantola, A. (2006), Popper, Bayes and the inverse problem, *Nature Physics*, **2**, 492-494.